

# The anti-apoptotic effect on cancer-associated fibroblasts of B7-H3 molecule enhancing the cell invasion and metastasis in renal cancer

This article was published in the following Dove Press journal:  
*OncoTargets and Therapy*

Shuai Zhang<sup>1,2</sup>  
Chenchao Zhou<sup>3</sup>  
Dongze Zhang<sup>1,2</sup>  
Ziyi Huang<sup>1,2</sup>  
Guangbo Zhang<sup>1,2</sup>

<sup>1</sup>Institute of Clinical Immunology, The First Affiliated Hospital of Soochow University,

<sup>2</sup>Jiangsu Institute of Jiangsu key Laboratory of Clinical Immunology, Soochow University; <sup>3</sup>Department of Urology, The First Affiliated Hospital of Soochow University, Suzhou 216007, People's Republic of China

**Background:** Renal cancer is one of the most common malignancies. However, the mechanisms underlying its development are still ambiguous. B7-H3 has been described as an important tumor antigen in various human tumors. An abnormal high expression of B7-H3 molecules is often observed in tumor cells and tumor stromal cells in the tumor microenvironment. On the basis of the above findings, we hypothesized that cancer-associated fibroblasts (CAFs) clustered in the renal cell microenvironment can survive for a long time with the anti-apoptotic effect of B7-H3, and then secrete cytokines to enhance the malignant behavior of renal cancer cells.

**Methods:** The expression of B7-H3 protein in CAFs was detected in renal cancer tissues. Then, the CAFs cells were stably transfected with shRNA and their expression was silenced to determine the role of B7-H3 in CAFs. Western blot was used to detect the expression of apoptosis-related proteins, hepatocyte growth factor (HGF) protein and stromal cell-derived factor-1 (CXCL12) protein. CAF-NC cells and CAFs-shRNA cells were co-cultured with A498 cells to assess the biological function changes of A498.

**Results:** A group of CAFs were found with B7-H3 expression in renal cancer. B7-H3 can stimulate CAFs to secrete HGF and Cxcl-12, and has strong anti-apoptotic effect on CAFs. We also found that CAFs-NC promotes the proliferation, invasion and migration of A498 cells in vitro and promotes the tumor formation of A498 in vivo.

**Conclusion:** B7-H3<sup>+</sup> CAFs promote the invasion and metastasis in renal cancer.

**Keywords:** renal cancer, tumor microenvironment, cancer-associated fibroblasts, B7-H3, apoptosis, invasion, metastasis

## Introduction

The B7-H3 molecule has two subtypes, 2IgB7-H3 and 4Ig B7-H3, and the human B7-H3 molecule includes both subtypes, with 4IgB7-H3 as the predominant subtype in human tissues.<sup>1</sup> Northern blot analysis revealed that B7-H3 is encoded by 4.1 kb mRNA, which is widely expressed in human tissues, but is limited in B7-H3 protein expression.<sup>2</sup> There is an aberrant expression of B7-H3 molecules in both tumor cells and interstitial cells.<sup>3-8</sup> cancer-associated fibroblasts (CAFs) are mainly derived from five types of cells,<sup>9-11</sup> mainly expressing  $\alpha$ -smooth muscle actin, vimentin and fibroblast activation protein,<sup>12</sup> which are the main components of host cells in the tumor microenvironment.<sup>13</sup> Several studies have highlighted that CAFs can enhance tumor proliferation, invasion and metastasis by means of releasing multiple cytokines.<sup>14-17</sup>

Correspondence: Guangbo Zhang  
Institute of Clinical Immunology, The First Affiliated Hospital of Soochow University, 708 Renmin Road, Jiangsu Province, Suzhou 216007, People's Republic of China  
Tel +8615895563791  
Email suzhouzhangguangbo@hotmail.com

Renal cancer is a relatively common malignant carcinoma, accounting for 2–3% of adult malignant tumors.<sup>18,19</sup> A distinctly worrying statistic revealed that approximately 20–30% of patients are found to have distant metastases when initially diagnosed with renal cancer.<sup>20,21</sup> The currently existing treatment options for renal cancer have low sensitivity toward radiotherapy and chemotherapy, leaving patients with high risk of recurrence following surgery and therefore the overall survival rate of patients with renal cancer remains low.<sup>22,23</sup> Due to the above dilemma, there is an urgent need in finding a new and improved therapeutic approach in forms of tumor gene therapy or immunotherapy for the treatment of kidney cancer.

Previous studies have linked the high expression of B7-H3 with an increase in the probability of tumor cell metastasis and increased chance of recurrence following surgery. At present, there is no research on the biological behavior and mechanism of B7-H3<sup>+</sup>CAFs on renal cancer cells. Our study used shRNA-mediated gene silencing to study the biological function of B7-H3 on CAFs, and further elucidated the progression of renal cell carcinoma through changes in the biological function of CAFs.

## Methods

### Ethics statement

All related experiments had been approved and supervised by the Ethics Committee of the First Affiliated Hospital of Soochow University and all patients enrolled in the study had signed written informed consent. Each procedure was performed in strict accordance with the Declaration of Helsinki. The animal experiment is in strict accordance with the “Guiding Opinions on the Treatment of Experiment of Animal” and the “Administrative Measures for Laboratory Animals in Jiangsu Province.”

### Tumor tissue samples

Ten renal cancer tissue specimens were obtained via radical nephrectomy at the First Affiliated Hospital of Soochow University between June 2016 and August 2016. None of the patients received preoperative chemotherapy or radiotherapy before the surgery. All patients were confirmed by pathological diagnosis.

### Preparation of single cell suspension of renal cancer tissue

Fresh renal cancer tissue was placed in a six-well plate, and washed with PBS (HyClone, USA) for the removal of

blood clots, fat and capsule. After additional rinsing, the tissue samples were cut with scissors, followed by the removal of PBS and the addition of type IV collagenase solution 2 mL (Thermo Fisher Scientific, USA). The six-well plate was incubated under 37°C, in CO<sub>2</sub> incubator for 1.5 hrs, followed by the addition of 1 mL of medium to stop digestion. A 300-mesh stainless steel filter sieve was placed in the culture dish, and the tissue in the well was transferred to a filter sieve for thorough grinding, followed by rinsing with PBS. The filtrate was filtered to a centrifuge tube, filtered through a cell sieve, centrifuged for 5 mins then discarded. The supernatant was removed, and the lower layer pellet was resuspended in PBS to 1 mL and stored in a refrigerator at 4°C.

### Cell culture

Human renal cancer cell line (A498) and CAFs cell line were purchased from the Chinese Academy of Sciences cell bank. RPMI1640 and DMEM high glucose medium (Gibco, USA) containing 10% FBS (Gibco, USA) and 1% penicillin and Streptomycin (Beyotime, People's Republic of China) mixture, respectively, cultured in a 37°C, 5% saturated humidity incubator.

### Flow cytometry for detection of CD29 and B7-H3 (CD276) expression in renal cell carcinoma tissue

50 µL of tumor cell suspension in the flow tube of No. 1–5 was added to flow antibody 2 µL, respectively. The entire process was performed on ice. The flow scheme was conducted as follows: tube No. 1 was the blank control tube, tube No. 2 was added to PE/Cy7 CD45, tube No. 3 was added to APC CD29, tube No. 4 was added to PE/Cy7 CD45+APC CD29 and tube No. 5 was added to PE/Cy7 CD45+APC CD29+PE CD276 (Biolegend, USA). Once each tube was thoroughly blown, incubation was carried out in a refrigerator at 4°C for 30 mins. The flow tube was removed, and each tube was added with 1 mL of PBS, and centrifuged, with the supernatant discharged, and resuspended to 500 µL with PBS, and detected by flow cytometry.

### Cell transfection

The silencing of B7-H3 sequences was designed by Shanghai GeneChem Co. Ltd. (Shanghai, People's Republic of China) and hU6-MCS-Ubiquitin-EGFP-IRES-puromycin as plasmid vector. Endogenous B7-H3 expression in CAFs

cells was knocked down with siRNA with the following target sequence: the sense sequence is 5-GUGCUG-GAGAAAGAUCAAATT-3, and the anti-sense sequence is 5-UUUGAUCUUUCUCCAGCACTT-3. The cells were seeded in 6-well plates, 24 hrs after the cell attachment, the virus liquid was mixed in the culture medium. The cells were screened with puromycin dihydrochloride (2 µg/mL; Amresco, USA) 72 hrs later. After 3 days post-transfection, 90% of the cells were transfected by observing the expression of green fluorescent protein (GFP)P. There were respective two experimental groups for CAFs cells: cells transfected with lentivirus-mediated shRNA-targeted B7-H3 were named CAFs-shRNA cells, while cells transfected with lentivirus-mediated shRNA (negative control, NC) were named CAFs-NC cells.

### CAFs-shRNA cell proliferation assay

The differences in proliferation between CAFs-shRNA and CAFs-NC cells were determined by CCK8 assay (Dojindo, Japan). The two groups of cells were inoculated into a 96-well plate at  $4 \times 10^3$  cells/well, and cultured in a 37°C, 5% saturated humidity incubator. The OD values were measured at four different time points at 0, 24, 48 and 72 hrs at 450 nm.

### CAFs-shRNA cell apoptosis and cycle assay

Apoptosis detection was performed using the Annexin V-PE Apoptosis Detection Kit (BD, USA). CAFs-shRNA and CAFs-NC cells were infected for 1 week, trypsinized, centrifuged, resuspended in PBS, stained with Annexin V-PE/PI and detected by flow cytometry. Cell cycle assays were performed using a PI staining kit (BD, USA). Cellular DNA content was detected on the basis of the relative proportion of cells at the G1/G0, S, and G2/M phases of the cell cycle.

### Western blot

CAFs-shRNA cells and CAFs-NC cells were separately added to 100 µL of lysate (Beyotime, People's Republic of China) for 30 mins on ice, after which centrifugation was conducted at 4°C to obtain the supernatant. The supernatant was then mixed with SDS protein loading buffer at 100°C for 10 mins. Next, a 30 µg protein sample was electrophoresed on 10% SDS-PAGE gel and transferred onto a PVDF membrane. The PVDF membrane was blocked with 5% skim milk prepared in TBST for 1 hr at

room temperature, and incubated with a specific primary antibody, including B7-H3, Bcl-2, Bax, Apaf1, cytochrome C, caspase-3, P-AKT, AKT, cyclin D1 (CST, USA) overnight at 4°C. Subsequently, three wash sessions were performed using TBST (5 mins each time). Horseradish peroxidase (HRP)-conjugated secondary antibody was incubated for 1 hr at room temperature, with the membrane washed and developed accordingly.

### Real-time PCR

After 2 weeks of culture of CAFs-shRNA cells and CAFs-NC cells, total RNA was extracted from each group of cells using Trizol (Beyotime, People's Republic of China), with the absorbance ratio of the sample RNA measured at wavelengths of 260 and 280 nm. The purity and concentration were then measured. Reverse transcription of RNA into cDNA was performed using the Takara Reverse Transcription Kit, 20 µl system, with the target gene detected by real-time PCR.

### A498 cell proliferation assay

The effects of CAFs-shRNA and CAFs-NC cells on the proliferation of the A498 cells were determined using a CCK8 assay. The lower chamber of Transwell 96-well plate was inoculated with A498 at  $4 \times 10^3$  cells/well, and  $1.0 \times 10^4$  CAFs-shRNA and CAFs-NC cells were added to the upper chamber, and cultured at 37°C in a 5% saturated humidity incubator. The absorbance was measured at 450 nm at 0, 24, 48 and 72 hrs.

### Invasion and migration assay

During the migration test, CAFs-shRNA and CAFs-NC cells were inoculated into the Transwell (Corning, USA) lower chamber at  $2.5 \times 10^4$  cells/well overnight. Then, the culture medium was replaced with serum-free medium the next day. Renal cell carcinoma cells were diluted to  $1 \times 10^6$  cells/mL in serum-free medium, with 200 µL added to the upper chamber. After incubation in a 37°C incubator for 24 hrs, 5% paraformaldehyde was used to fix the chamber for 15 mins. Crystal violet staining was performed over a period of 10 mins, with the cells failing to pass wiped with a cotton ball. Five fields were taken from the top, bottom, left and right of the microscope, photographed and statistically analyzed. During the invasion test, CAFs-shRNA and CAFs-NC cells were inoculated into the Transwell lower chamber at  $2.5 \times 10^4$  cells/well. Matrigel (Corning, USA) was pre-plated on the bottom membrane of the upper chamber. The A498 cell suspension was then added, and cultured at 37°C in an

incubator for 24 hrs. The cells were fixed and stained. With five fields of view from top to bottom, left and right obtained, the cells were photographed, and analyzed statistically.

## Tumor growth in vivo

CAFs-shRNA cells and CAFs-NC cells ( $1.0 \times 10^6$  cells) were mixed with A498 cells ( $1.0 \times 10^6$  cells), respectively, and subcutaneously injected into 8-week-old male BALB/c nude mice. There were a total of eight mice, with 4 mice in each group. Tumor size was recorded every 3 days. The tumors were collected approximately 6 weeks after injection.

## Statistical analysis

Mapping and data analyses were performed using Flowjo-V10, GraphPad Prism 7.0 and SPSS 23 statistical software. Experimental data were expressed as mean $\pm$ SD. The mean comparison between the two groups was performed by two-tailed Student's *t*-test with  $p < 0.05$  considered as statistically significant.

## Results

### CAFs expressing B7-H3 molecules were found in renal cell carcinoma tissue

CD45-negative and CD29-positive were used for flow cytometry in order to demonstrate the presence of a panel of B7-

H3 expressing fibroblasts in renal cell carcinoma. The flow cytometric analysis of single-cell suspensions of renal cell carcinoma revealed that there is a group of B7-H3<sup>+</sup>CAFs among the renal cell carcinoma tissues (Figure 1).

### Transfection efficiency verification

After transfecting CAFs cells with B7-H3-shRNA and negative control virus, green fluorescence was observed in the cytoplasm. The results obtained from fluorescence microscopy showed that the transfection efficiencies of the B7-H3-shRNA and negative control virus, which both exceeded 90%, were satisfactory (Figure 2A). Flow cytometry was used to detect B7-H3 protein in CAFs cells for assessing whether B7-H3-shRNA effectively silences B7-H3 expression in CAF cells. As shown in Figure 2B, the expression of B7-H3 protein in the experimental group was 14.4%. Subsequently, total protein was extracted from CAFs cells, and B7-H3 expression in cell lysates was analyzed by Western blot. As shown in Figure 2C, a significant decrease in B7-H3 protein expression was observed after transfection with B7-H3-shRNA in comparison to the cells from the control group. Simultaneously, the expression level of B7-H3 mRNA was lower than that of the CAFs-NC group (Figure 2D). Therefore, the CAFs-shRNA stable line, named CAF-shRNA cells, was used for further analysis.

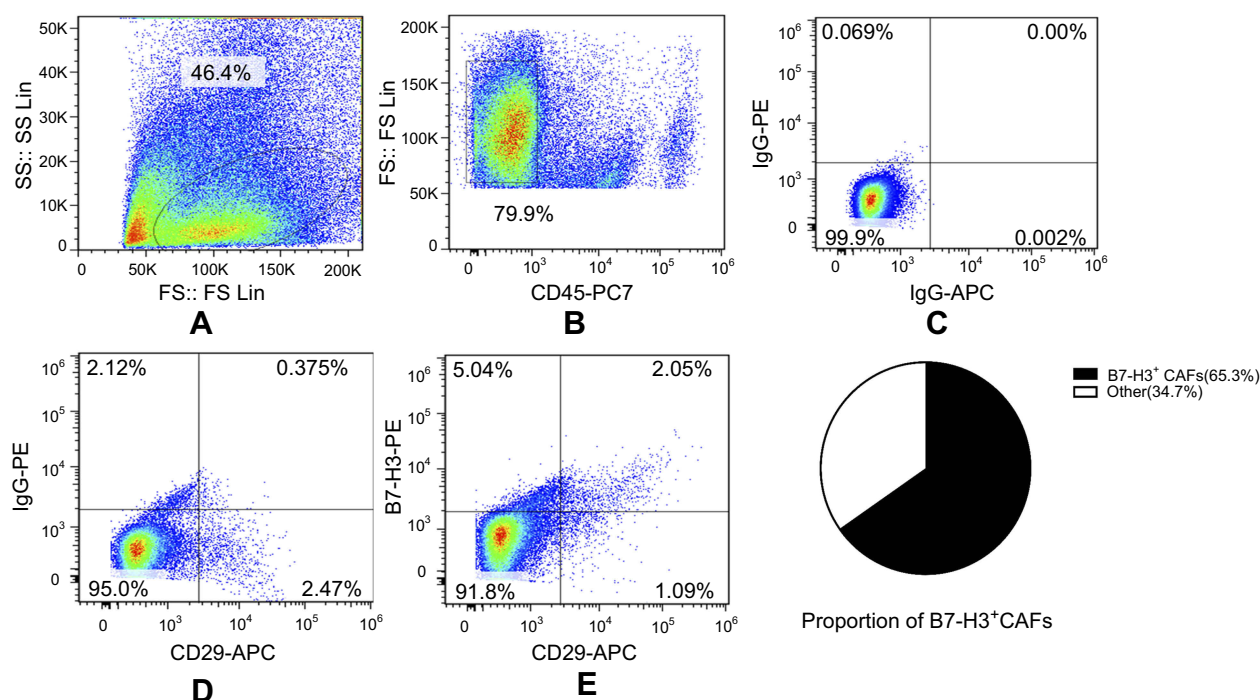


**Figure 1** Flow cytometric analysis of cell surface B7-H3 expression levels of CAFs in renal cell carcinoma. (A) FS-SS scatter plot to circle large cell populations and remove dead cells; (B) circle out cell populations that do not express CD45; (C, D) Isotype control; (E) the double positive region is B7-H3<sup>+</sup>CAFscells, which is about 65.3%.



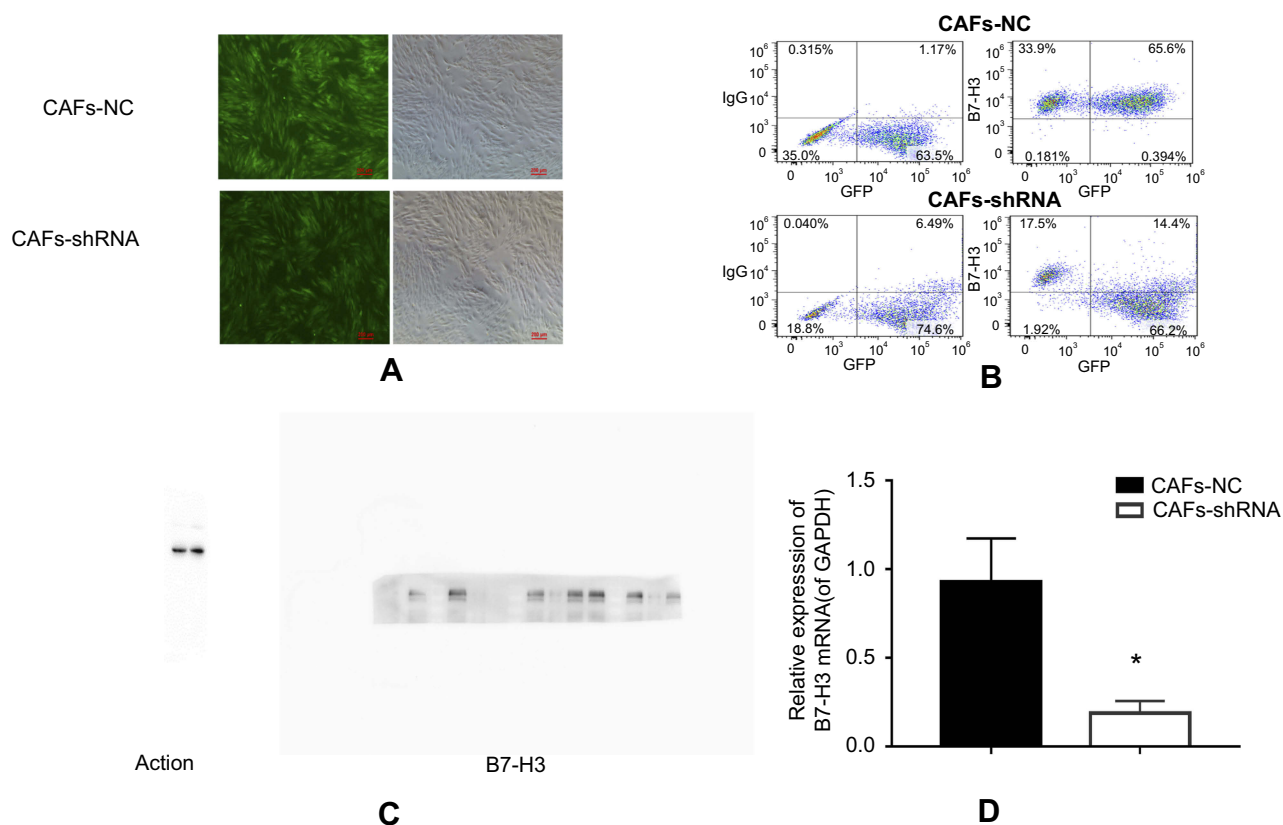


**Figure 2** (A) The transfection efficiencies observed of cancer-associated fibroblasts (CAFs) using fluorescence microscopy; (B) B7-H3 expression levels detected in CAFs by flow cytometry; (C) B7-H3 expression levels in CAFs detected by Western blot; (D) B7-H3 mRNA level determined by Q-PCR. \* $p < 0.05$ .

## B7-H3 silencing reduced CAFs cell proliferation and induces apoptosis

CCK-8 assay was performed for the detection of the potential effect of RNAi-mediated downregulation of B7-H3 on CAFs cell growth. In Figure 3A, the results show that CAFs-shRNA cell growth rate is significantly reduced on day 2 as compared to CAFs-NC cells ( $p < 0.01$ ). In Figure 3B, flow cytometry analysis results revealed that CAFs-shRNA cells were arrested at the G0/G1 phase of the cell cycle in comparison to CAFs-NC cells ( $52.391 \pm 0.923$  and  $24.446 \pm 0.698$ ,  $p < 0.01$ ). The percentage of S + G2/M phase in CAFs-shRNA cells was lower than that in CAFs-NC cells ( $44.353 \pm 2.601$  and  $79.121 \pm 4.502$ ,  $p < 0.01$ ). These results demonstrated that in the event that B7-H3 expression was decreased, the percentage of G0/G1 increased and the proportion of S+G2/M was decreased. Those findings suggested that B7-H3 gene silencing resulted in G0/G1 arrest and ultimately inhibiting CAFs proliferation. At the same time, Annexin V-PE/PI double staining was applied to detect apoptosis. The percentage of early apoptosis of CAFs-shRNA was higher

than that of CAFs-NC ( $25.567 \pm 7.023$  and  $4.083 \pm 1.499$ ,  $p < 0.05$ ). There was no significant difference regarding the apoptosis rate between the two groups ( $2.187 \pm 1.007$  and  $4.243 \pm 0.996$ ,  $p > 0.05$ ). The experimental data suggested that downregulation of B7-H3 expression could potentially induce CAF apoptosis.

## Changes in genes and related protein molecules after B7-H3 silencing

The changes that occurred following the silencing of B7-H3 molecules by gene chip method were analyzed in signaling molecules in CAF cells. Based on the findings, B7-H3 signal could potentially lead to the upregulation of 4,531 genes and the downregulation of 3,677 genes (Figure 4A). Compared with the control group (NC), many signal molecules were changed in the experimental group. For example, the expressions of *p-akt*, *bcl-2*, *cyclin D1* and *HGF* were downregulated and the expressions of *Bad* and *caspase-3* were upregulated. Based on these results, we conducted further experiments to determine the underlying molecular mechanism by which B7-H3 signaling confers its anti-apoptotic effect.

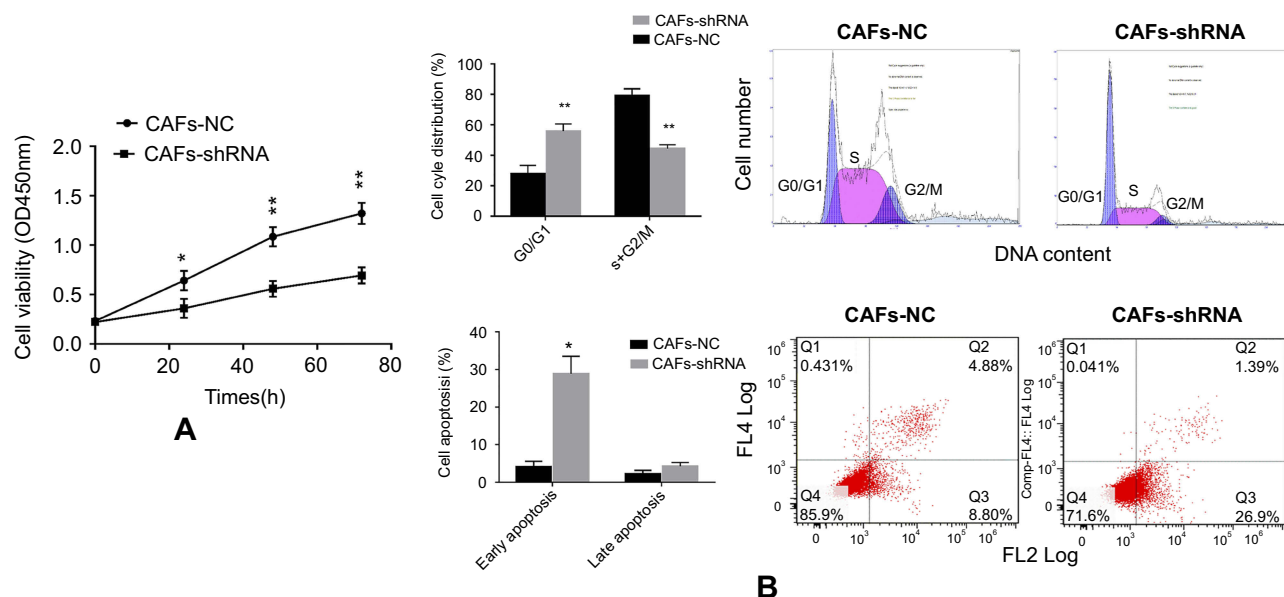


**Figure 3** Silencing B7-H3 reduces cancer-associated fibroblasts (CAFs) proliferation and induces apoptosis. **(A)** Viability measured by cck8 assay in CAFs cells; **(B)** cell cycle distribution and cell apoptosis of CAFs cells were identified by flow cytometry. \* $P < 0.05$ ; \*\* $P < 0.01$ .

To further investigate the composition of B7-H3 gene silencing on CAF apoptosis and the periodic signaling pathway, Western blot analysis was performed to detect apoptosis and expression of cell cycle-related proteins. The results revealed that there was an increase in pro-apoptotic Bax, decrease of anti-apoptotic Bcl-2 and cell cycle associated cyclin D1, decrease of Apaf-1 and cytochrome C, and activation of caspase-3 all in comparison to controls. Furthermore, the knockdown of B7-H3 decreased AKT phosphorylation, but did not affect total AKT protein expression level in CAFs-shRNA cells (Figure 4B).

## A link of CAFs-shRNA to tumor cell proliferation, migration and invasion

CCK-8 assay was performed to detect the effect of CAFs-shRNA on the proliferation of A498 cells. As shown in Figure 5B, the proliferation of CAFs-shRNA+A498 cells was significantly reduced ( $p < 0.05$ ) compared to that of CAFs-NC+A498 cells. Next, Transwell method was used to evaluate the effect of CAFs-shRNA on A498 migration and invasion. As shown in Figure 5C, the migration and invasion ability of CAFs-shRNA cells of A498 was lower than that of CAFs-NC cells ( $p < 0.05$ ). These findings suggested that CAFs-NC promotes motility and invasion of A498 cells. A xenograft tumor model of BALB/c nude mice was established by injecting stable CAFs-shRNA +A498 cells and CAFs-NC+A498 cells into the bare groin

to confirm the function of B7-H3 in vivo renal cancer. The size of the tumor volume is shown in Figure 5D. The results showed that the tumor volume of nude mice injected with CAFs-shRNA+A498 cells was smaller than that of nude mice injected with CAFs-NC+A498 cells ( $p < 0.001$ ). Our data indicate that silencing of the B7-H3 gene on CAFs leads to inhibition of tumor growth. After Western blot analysis, we observed a decrease in hepatocyte growth factor (HGF) protein and stromal cell-derived factor-1 (CXCL12) protein relative to controls (Figure 5A).

## Discussion

As an immunomodulatory molecule, B7-H3 plays multiple roles in different types of human tumors.<sup>24</sup> Moreover, the role of B7-H3 in tumor immunity is complex due to the co-stimulatory and co-suppressive effects of T cells.<sup>25,26</sup> The present study was conducted with the main focus on the association between B7-H3<sup>+</sup>CAFs and tumor progression in renal cancer.

In this study, we first explored the effects of B7-H3 on the biological function of CAFs. According to the results, B7-H3 gene silencing significantly inhibits cell proliferation, increases apoptosis, inhibits cell cycle, and decreases expression of HGF protein and stromal cell-derived factor-1 (Cxcl12) protein. Previous study has confirmed that CAFs can promote tumor cell proliferation, invasion, metastasis and angiogenesis.<sup>27</sup> CAFs apoptosis could provide

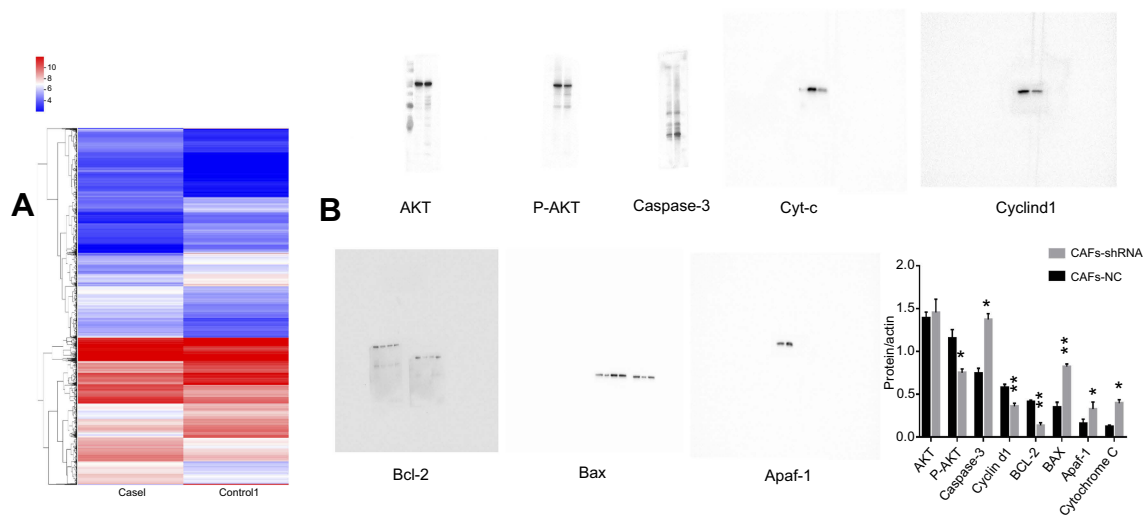


**Figure 4 (A)** Silencing B7-H3 molecular expression leads to differential gene expression analysis in cancer-associated fibroblasts (CAFs ); **(B)** B7-H3 regulates protein expression levels of apoptosis-related proteins.

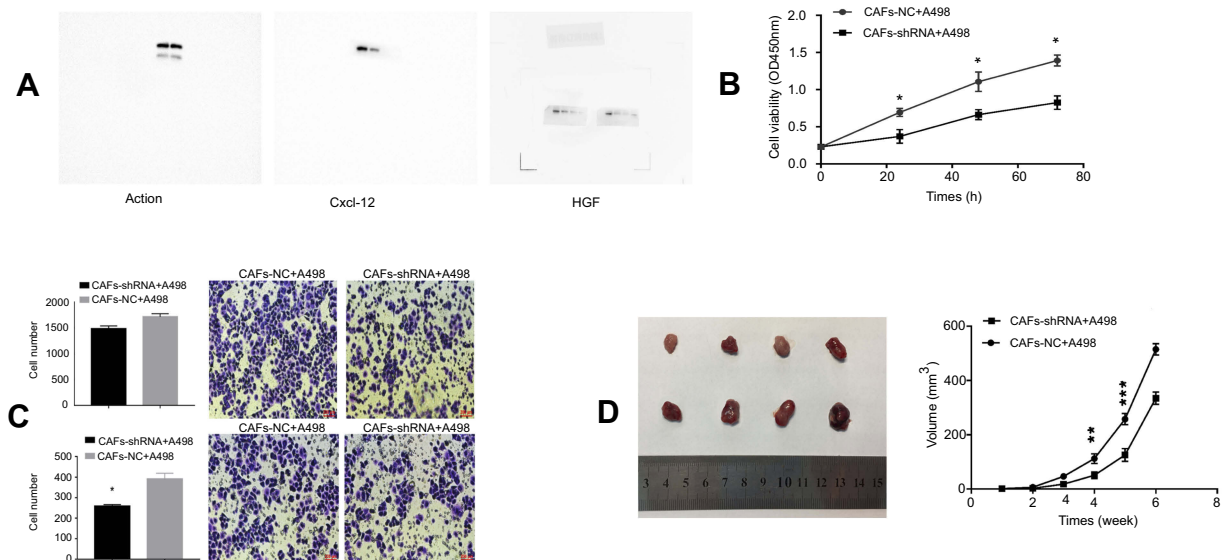


**Figure 5** Effect of cancer-associated fibroblasts (CAFs)-shRNA on proliferation, migration and invasion of A498 cells. **(A)** B7-H3 regulates protein expression levels of hepatocyte growth factor (HGF) protein and stromal cell-derived factor-1 (CXCL12) protein; **(B)** CAFs-shRNA cells inhibit the proliferation of A498 cells; **(C)** CAFs-shRNA reduces migration and invasion of A498 cells; **(D)** effect of CAFs-shRNA on renal cell carcinoma in vivo. \* $P < 0.05$ ; \*\* $P < 0.01$ ; \*\*\* $P < 0.001$ .

a therapeutic option for tumors based on previous studies, Bcl-2 blocks apoptosis by preventing pro-apoptotic molecules from mitochondria into the cytosol, while Bax promotes apoptosis by inducing mitochondrial outer membrane permeabilization.<sup>28–30</sup> Bax/Bcl-2 ratio controls the ultimate sensitivity to cell death stimuli.<sup>31</sup> Apaf-1 plays an important role in the mitochondrial pathway, as it facilitates several processes, including the formation of apoptotic bodies with cytochrome C and dATP, activation of caspase-3 and inducing cell apoptosis.<sup>32</sup> Our study found that the transfection of CAFs cells with B7-H3-shRNA results in a decrease in the

anti-apoptotic protein Bcl-2, while increasing the pro-apoptotic protein Bax and the Apaf-1 protein and cytochrome C protein. An increase in level of pro-apoptotic proteins and/or decreased anti-apoptotic proteins could lead to apoptosis. Moreover, there exist complex links between cell cycle and cell apoptosis. Generally, cell cycle arrest is followed by the apoptosis of cells.<sup>33</sup> In the present study, B7-H3 gene silencing blocked the conversion of cyclin D1 from G0/G1 to S and G2/M, and decreased cyclin D1 expression.

The effect of B7-H3<sup>+</sup>CAFs on the aggressive behavior of renal cell carcinoma cell line (A498) was explored. Our

in vitro demonstrated that B7-H3<sup>+</sup>CAFs plays a significant role in tumor growth and metastatic progression. The orthotopic xenograft tumor model of nude mice was also established to further confirm the effect of B7-H3<sup>+</sup>CAFs on the growth of tumors in vivo. The results indicated that CAFs-shRNA facilitates the decline in growth rate of xenografts in vivo and has a potent therapeutic effect against tumor cells. Western blot analysis showed that the expression of HGF protein and stromal cell-derived factor-1 (Cxcl-12) protein decreased as compared with the control group. Previous study has reported that CAFs could secrete HGF and promote tumor development.<sup>34</sup> Simultaneously, Cxcl-12 secreted by CAFs binds to CXCR4 and mediates cancer cell growth and mitosis through transcription-dependent or non-transcription-dependent pathways, promoting cell proliferation and invasion and metastasis.<sup>35–37</sup>

The AKT pathway plays a significant role in several biological functions in various human cancers. The downregulation of AKT expression could inhibit tumor cell proliferation and increase apoptosis,<sup>38</sup> while the downstream targets of AKT have been identified as the molecules correlated with apoptosis, such as Bcl-2 and caspase-3.<sup>39</sup> The increase of AKT activation and apoptosis protein could increase the permeability of mitochondrial membrane.<sup>40</sup> The combination of cytochrome C and apaf-1 stimulated the activation of caspase-3.<sup>32</sup> In this study, B7-H3-shRNA induced B7-H3 gene silencing inhibited AKT phosphorylation. We also found that inhibition of AKT phosphorylation through the silencing of B7-H3 suggests that B7-H3 inhibition might be responsible for reducing the expression of HGF protein and Cxcl12 protein in CAFs cells through the AKT pathway, increasing apoptosis and preventing cell cycle process. These results suggest that there could be a potential correlation between B7-H3 and AKT signaling pathway.

In conclusion, this study found that B7-H3<sup>+</sup> CAFs are associated with tumor progression in renal cell carcinoma and might be a potential target for the treatment of human renal cell carcinoma in the future. However, our study had limitations due to lack of experimental funds and laboratory conditions. In addition, this study was performed in tumor-forming experiments, and there were no further animal experiments performed for further confirmation. Therefore, these key points, along with the specific molecular mechanism of B7-H3, are worth exploring in future studies on a larger scale.

## Acknowledgments

This study was supported by the National Natural Science Foundation of China (NO.81872328); Major Project of Natural Science Research of Jiangsu Provincial Department of Education (NO.17KJA310004).

## Disclosure

The authors report no conflicts of interest in this work.

## References

- Steinberger P, Majidic O, Derdar SV, et al. Molecular characterization of human 4Ig-B7-H3, a member of B7 family with four Ig-like domains. *The Journal of Immunol.* 2004;172:2352–2359. doi:10.4049/jimmunol.172.4.2352
- Alderson MR, Craig AS, Tercsa WT, et al. Molecular and biological characterization of human 4-1bb and its ligand. *Eur J Immunol.* 1994;24:2219–2227. doi:10.1002/eji.1830240943
- Zhang T, Jiang B, Zou S-T, et al. Overexpression of B7-H3 augments anti-apoptosis of colorectal cancer cells by Jak2-STAT3. *World J Gastroenterol.* 2015;21(6):1804–1813. doi:10.3748/wjg.v21.i6.1804
- Kang FB, Wang L, Li D, et al. Hepatocellular carcinomas promote tumor-associated macrophage M2-polarization via increased B7-H3 expression. *Oncol Rep.* 2015;33(1):274–282. doi:10.3892/or.2014.3587
- Jin Y, Zhang P, Li J, et al. B7-H3 in combination with regulatory T cell is associated with tumor progression in primary human non-small cell lung cancer. *Int J Clin Exp Pathol.* 2015;8(11):13987–13995.
- Dai W, Shen G, Qiu J, et al. Aberrant expression of B7-H3 in gastric adenocarcinoma promotes cancer cell metastasis. *Onco Rep.* 2014;32(5):2086–2092. doi:10.3892/or.2014.3405
- Sun J, Guo YD, Li XN, et al. B7-H3 expression in breast cancer and upregulation of VEGF through gene silence. *Onco Targets Ther.* 2014;7(6):1979–1986. doi:10.2147/OTT.S63424
- Yuan H, Wei X, Zhang G, Li C, Zhang X, Hou J. B7-H3 over expression in prostate cancer promotes tumor cell progression. *J Urol.* 2011;186(3):1093–1099. doi:10.1016/j.juro.2011.04.103
- Lawrenson K, Grun B, Lee N, et al. NPPB is a novel candidate biomarker expressed by cancer - associated fibroblasts in epithelial ovarian cancer. *Int J Cancer.* 2015;136(6):1390–1401. doi:10.1002/ijc.29092
- Sosulski ML, Gongora R, Danchuk S, Dong C, Luo F, Sanchez CG. Deregulation of selective autophagy during aging and pulmonary fibrosis: the role of TGFβ1. *Aging Cell.* 2015;14(5):774–783. doi:10.1111/ace.12357
- Sampson N, Brunner E, Weber A, et al. Inhibition of Nox4 - dependent ROS signaling attenuates prostate fibroblast activation and abrogates stromal - mediated protumorigenic interactions. *Int J Cancer.* 2018;143(2):383–395. doi:10.1002/ijc.31316
- Ishii G, Ochiai A, Neri S. Phenotypic and functional heterogeneity of cancer-associated fibroblast within the tumor microenvironment. *Adv Drug Deliv Rev.* 2016;99(Pt B):186–196.
- Nair N, Calle AS, Zahra MH, et al. A cancer stem cell model as the point of origin of cancer-associated fibroblasts in tumor microenvironment. *Sci Rep.* 2017;7(1):6838. doi:10.1038/s41598-017-07144-5
- Jeleszk C, Victor B, Podgorski I, Sloane BF. Fibroblast hepatocyte growth factor promotes invasion of human mammary ductal carcinoma in situ. *Cancer Res.* 2009;69(23):9148–9155. doi:10.1158/0008-5472.CAN-08-3660
- Augsten M, Hagglof C, Olsson E, et al. CXCL14 is an autocrine growth factor for fibroblasts and acts as a multi-modal stimulator of prostate tumor growth. *Proc Natl Acad Sci USA.* 2009;106(9):3414–3419. doi:10.1073/pnas.0813144106



16. Lederle W, Hartenstein B, Meides A, et al. MMP13 as a stromal mediator in controlling persistent angiogenesis in skin carcinoma. *Carcinogenesis*. 2010;31(7):1175–1184. doi:10.1093/carcin/bgp248
17. Kalluri R, Zeisberg M. Fibroblasts in cancer. *Nat Rev Cancer*. 2016;6(5):3, 92–401.
18. Cairns P. Renal cell carcinoma. *Cancer Biomark*. 2010;9(1–6):461–473. doi:10.3233/CBM-2011-0176
19. Rebecca L, Siegel MPH, Kimberly D, Miller MPH, Ahmedin Jemal DVM. Cancer statistics. *Ca Cancer J Clin*. 2018;68:7–30.
20. Jiang Z, Chu PG, Woda BA, et al. Combination of quantitative IMP3 and tumor stage: a new system to predict metastasis for patients with localized renal cell carcinomas. *Clin Cancer Res*. 2008;14(17):5579–5584. doi:10.1158/1078-0432.CCR-08-0504
21. Scherr AJ, Lima JP, Sasse EC, et al. Adjuvant therapy for locally advanced renal cell cancer: a systematic review with meta-analysis. *BMC Cancer*. 2011;11:115. doi:10.1186/1471-2407-11-115
22. Jonasch E, Futreal A, Davis I, et al. State-of-the-science: an update on renal cell carcinoma. *Mol Cancer Res*. 2012;10(7):859–880. doi:10.1158/1541-7786.MCR-12-0117
23. Patil S, Ishill N, Deluca J, Motzer RJ. Stage migration and increasing proportion of favorable-prognosis metastatic renal cell carcinoma patients: implications for clinical trial design and interpretation. *Cancer*. 2010;116(2):347–354. doi:10.1002/cncr.v116:2
24. Wang Z-S, Zhong M, Bian Y-H, et al. MicroRNA-187 inhibits tumor growth and invasion by directly targeting CD276 in colorectal cancer. *Oncotarget*. 2016;7:44266–44276.
25. Zhang G, Chen Y, Shi Q, et al. Human recombinant B7-H3 expressed in *E coli* enhances T lymphocyte proliferation and IL-10 secretion in vitro. *Acta Biochim Biophys Sin(Shanghai)*. 2004;36:430–436.
26. Ling V, Wu PW, Spaulding V, et al. Duplication of primate and rodent B7-H3 immunoglobulin V- and C-like domains: divergent history of functional redundancy and exon loss. *Genomics*. 2003;82:365–377.
27. Cirri P, Chiarugi P. Cancer associated fibroblasts: the dark side of the coin. *Am J Cancer Res*. 2011;1(4):482–497.
28. Tait SW, Green DR. Mitochondria and cell death: outer membrane permeabilization and beyond. *Nat Rev Mol Cell Biol*. 2010;11(9):621–632. doi:10.1038/nrm2952
29. Wang X. The expanding role of mitochondria in apoptosis. *Genes Dev*. 2001;15(22):2922–2933.
30. Liu Q, Chi X, Leber B, et al. Bcl-2 family and their therapeutic potential. In: Wu H, editor. *Cell Death: Mechanism and Disease*. New York (NY): Springer New York; 2013;61–96.
31. Reed JC. Dysregulation of programmed cell death in cancer toward a molecular understanding of Bcl-2. In Mihich E, Croce C, editors. *The Biology of Tumors*. Boston (MA): Springer US; 1998;145–171.
32. Yun T, Yu K, Yang S, et al. Acetylation of p53 at lysine 120 upregulates Apaf1 and sensitizes mitochondrial apoptotic pathway. *J Biol Chem*. 2016;291(1):7386–7395. doi:10.1074/jbc.M115.706341
33. Meikrantz W, Schlegel R. Apoptosis and the cell cycle. *J Cell Biochem*. 1995;58:160–174. doi:10.1002/jcb.240580108
34. Kumar D, New J, Vishwakarma V, et al. Cancer-associated fibroblasts drive glycolysis in a targetable signaling loop implicated in head and neck squamous cell carcinoma progression. *Cancer Res*. 2018;78(14):3769–3782. doi:10.1158/0008-5472.CAN-17-1076
35. Roy I, Zimmerman NP, Mackinnon AC, et al. Cxcl12 chemokine expression suppresses human pancreatic cancer growth and metastasis. *PLoS One*. 2014;9(3):e90, 400. doi:10.1371/journal.pone.0090400
36. Zhong W, Chen W, Zhang D, et al. CXCL12/CXCR4 axis plays pivotal roles in the organ specific metastasis of pancreatic adenocarcinoma: a clinical study. *Exp Ther Med*. 2012;4(3):363–369. doi:10.3892/etm.2012.719
37. Feig C, Jones JO, Kraman M, et al. Targeting CXCL12 from FAP-expressing carcinoma-associated fibroblasts synergizes with anti-PD-L1 immunotherapy in pancreatic cancer. *Proc Natl Acad Sci*. 2013;110(50):20212–20217. doi:10.1073/pnas.1320318110
38. Yuan Y, Du W, Wang Y, et al. Suppression of AKT expression by miR-153 produced anti-tumor activity in lung cancer. *Int J Cancer*. 2015;136(6):1333–1340. doi:10.1002/ijc.29103
39. Shi M, Zhang H, Li M, et al. Normal endometrial stromal cells regulate survival and apoptosis signaling through PI3K/Akt/Survivin pathway in endometrial adenocarcinoma cells in vitro. *Gynecol Oncol*. 2011;123:387–392. doi:10.1016/j.ygyno.2011.07.004
40. Datta SR, Dudeck RH, Tao X, et al. AKT phosphorylation of BAD couples survival signals to the cell-intrinsic death machinery. *Cell*. 1997;91(2):231–241. doi:10.1016/S0092-8674(00)80405-5

## OncoTargets and Therapy

### Publish your work in this journal

OncoTargets and Therapy is an international, peer-reviewed, open access journal focusing on the pathological basis of all cancers, potential targets for therapy and treatment protocols employed to improve the management of cancer patients. The journal also focuses on the impact of management programs and new therapeutic

agents and protocols on patient perspectives such as quality of life, adherence and satisfaction. The manuscript management system is completely online and includes a very quick and fair peer-review system, which is all easy to use. Visit <http://www.dovepress.com/testimonials.php> to read real quotes from published authors.

Submit your manuscript here: <https://www.dovepress.com/oncotargets-and-therapy-journal>

Dovepress